

Electronic Supporting Information

Smartphone-based digitized recognition of As³⁺ along with its effectual mitigation in water by a benzothiazole functionalized molecular scaffold

SomritaNag,^{a,b} AmitaMondal,^{a,c} Harish Hirani,^{a,d} PriyabrataBanerjee^{a,b*}

a. CSIR-Central Mechanical Engineering Research Institute, M. G. Avenue, Durgapur 713209, India. E-mail addresses: pr_banerjee@cmeri.res.in, Priyabrata_banerjee@hotmail.com, Webpage: www.cmeri.res.in and www.priyabratabanerjee.in

b. Academy of Scientific and Innovative Research (AcSIR), AcSIR Headquarters CSIR-HRDC Campus, Postal Staff College Area, Sector 19, Kamla Nehru Nagar, Ghaziabad-201002, Uttar Pradesh, India.

c. Department of Chemistry, National Institute of Technology, M. G. Avenue, Durgapur, 713209, India.

d. Mechanical Engineering Department, Indian Institute of Technology Delhi, New Delhi-110016, India.

Captions	Contents
Fig.S1.	Synthesis of ABH
Fig.S2.	ESI-Mass data and HRMS of ABH
Table S1	Crystallographic data of ABH
Table S2	Selected bond distances (angstrom) of ABH
Table S3	Selected bond angles (degrees) of ABH
Table S4	Hydrogen bonding in ABH
Fig.S3.	¹ H NMR data of ABH in DMSO-d ⁶ , 2D-COSY ¹ H NMR data of ABH in DMSO-d ⁶ and ¹³ CNMR of ABH in DMSO-d ⁶
Fig.S4.	Job's plot of ABH with As ³⁺
Fig.S5.	ESI-Mass data of ABH with As ³⁺
Fig.S6.	(a) B-H plot of ABH with As ³⁺ and (b) Ratio of absorbance of ABH with As ³⁺
Fig.S7.	Plots of Absorbance vs. Time of ABH with As ³⁺
Fig.S8.	(a) Absorbance spectra of ABH with different cations and (b) Interference of ABH with different cationic analytes in MeOH-H ₂ O
Fig.S9.	(a) UV-Vis spectra for Quantitative detection of As ³⁺ and (b) Schematic representation of phone coupled device fabrication for quantitative detection of As ³⁺
Fig.S10.	Sensing response of ABH after addition of As ³⁺ at different concentration presented in 3D-CAD model
Fig.S11.	Fabrication of the logic gate with outputs (Y1 and Y2) upon altering inputs of NAND–NOT–NOR logic functions for ABH with As ³⁺ and F ⁻
Fig.S12.	(a) Visual colour change of [ABH -As ³⁺] adduct with F ⁻ and other anions and (b) Reversibility ABH with As ³⁺ & F ⁻ in MeOH
Fig.S13, Table S5	Electrochemical response of ABH with As ³⁺ in MeOH
Fig.S14.	FT-IR spectra of ABH in solid state
Fig.S15.	FT-IR spectra of ABH +As ³⁺ in solid state
Table S6	Theoretical upshot of ABH :As ³⁺ interaction
Table S7	Cartesian coordinates of geometry optimized structure of ABH
Table S8	Cartesian coordinates of geometry optimized structure of ABH ...As ³⁺
Table S9	2D-COSY NMR
Table S10	Comparative literature study of ABH with other chemosensors

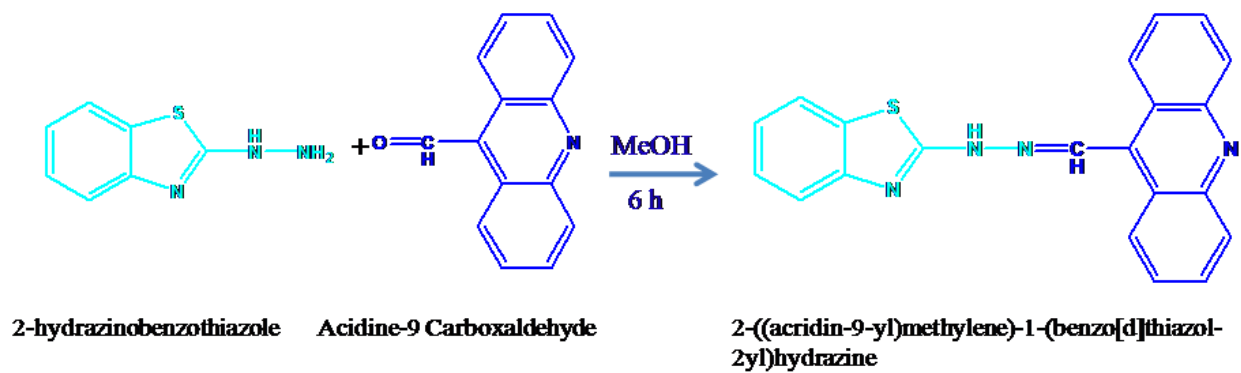


Fig.S1. Synthesis of ABH

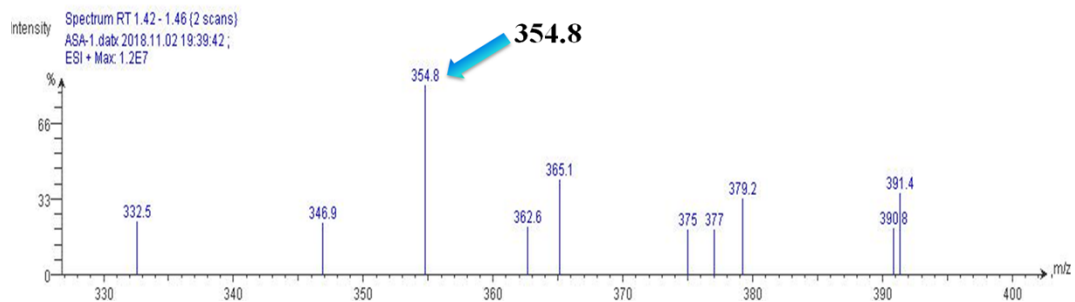


Fig.S2a. ESI-Mass data of ABH

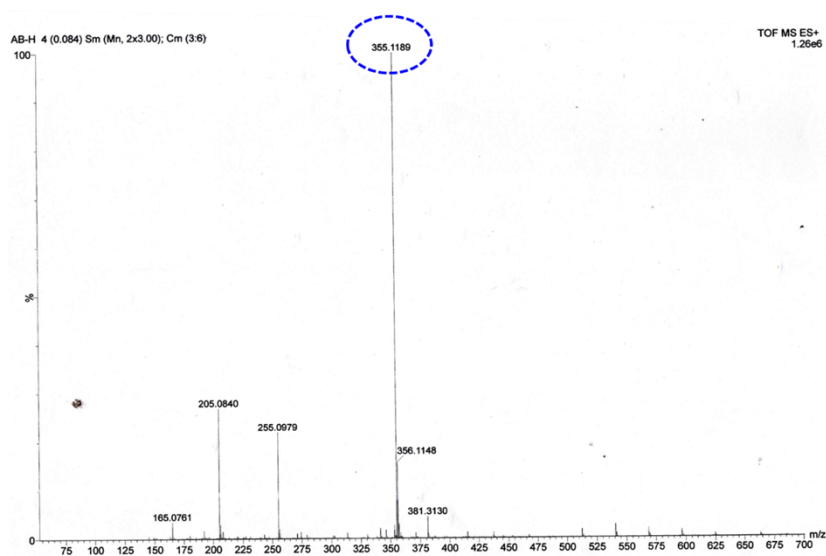


Fig.S2a. HR-MS data of ABH

Table S1 Crystallographic data of **ABH**

Crystal Data	
Formula	C ₂₁ H ₁₄ N ₄ S
Formula Weight	354.42
Crystal System	monoclinic
Space group	C2/c (No.15)
a, b, c [Angstrom]	27.201(7) 3.9233(10) 37.778(9)
alpha, beta, gamma [deg]	90 107.480(8) 90
V [Ang**3]	3845.4(17)
Z	8
D(calc) [g/cm**3]	1.224
Mu(MoKa) [/mm]	0.179
F(000)	1472
Crystal Size [mm]	0.10 x 0.11 x 0.12
Data Collection	
Temperature (K)	129
Radiation [Angstrom]	MoKa 0.71073
Theta Min-Max [Deg]	2.3, 25.0
Dataset	-32: 32 ; -4: 4 ; -44: 44
Tot., Uniq. Data, R(int)	13614, 3386, 0.102
Observed Data [I > 2.0 sigma(I)]	2179
Refinement	
Nref, Npar	3386, 235
R, wR2, S	0.0792, 0.1916, 1.03
w =	$\frac{1}{\sigma^2(F_o^2) + (0.0758P)^2 + 7.7249P}$ WHERE $P = \frac{(F_o^2 + 2F_c^2)}{3}$
Max. and Av. Shift/Error	0.00, 0.00
Min. and Max. Resd. Dens. [e/Ang^3]	-0.30, 0.29

Table S2 Selected bond distances (angstrom) of **ABH**

S001	-C009	1.752(5)	C00F	-C00N	1.432(6)
S001	-C00A	1.745(4)	C00G	-C00H	1.427(7)
N002	-C005	1.399(5)	C00H	-C00O	1.362(8)
N002	-C009	1.288(6)	C00I	-C00L	1.369(7)
N003	-N004	1.353(5)	C00J	-C00M	1.399(8)
N003	-C00D	1.284(5)	C00K	-C00M	1.374(7)
N004	-C009	1.360(5)	C00L	-C00O	1.394(8)
N006	-C00F	1.348(7)	C00N	-C00Q	1.347(8)
N006	-C00G	1.363(6)	C00P	-C00Q	1.399(7)
C005	-C00A	1.392(7)	C00C	-H00C	0.9500
C005	-C00C	1.389(6)	C00D	-H00D	0.9500
C007	-C00B	1.426(6)	C00E	-H00E	0.9500
C007	-C00E	1.441(7)	C00H	-H00H	0.9500
C007	-C00F	1.427(6)	C00I	-H00I	0.9500
C008	-C00B	1.422(6)	C00J	-H00J	0.9500
C008	-C00G	1.422(6)	C00K	-H00K	0.9500
C008	-C00I	1.424(6)	C00L	-H00L	0.9500
N004	-H004	0.8800	C00M	-H00M	0.9500
C00A	-C00K	1.391(6)	C00N	-H00N	0.9500
C00B	-C00D	1.460(6)	C00O	-H00O	0.9500
C00C	-C00J	1.378(7)	C00P	-H00P	0.9500
C00E	-C00P	1.348(6)	C00Q	-H00Q	0.9500

Table S3 Selected bond angles (degrees) of **ABH**

C009	-S001	-C00A	87.7(2)	N006	-C00F	-C007	123.5(4)
C005	-N002	-C009	109.6(4)	C007	-C00F	-C00N	120.0(4)
N004	-N003	-C00D	116.6(4)	N006	-C00F	-C00N	116.6(4)
N003	-N004	-C009	118.2(4)	N006	-C00G	-C00H	115.5(4)
C00F	-N006	-C00G	117.3(4)	C008	-C00G	-C00H	120.1(4)
N002	-C005	-C00A	115.1(4)	N006	-C00G	-C008	124.4(4)
N002	-C005	-C00C	125.4(4)	C00G	-C00H	-C00O	120.4(5)
C00A	-C005	-C00C	119.5(4)	C008	-C00I	-C00L	119.5(4)
C00B	-C007	-C00E	124.9(4)	C00C	-C00J	-C00M	120.3(4)
C00B	-C007	-C00F	118.7(4)	C00A	-C00K	-C00M	118.4(5)
C00E	-C007	-C00F	116.4(4)	C00I	-C00L	-C00O	123.0(5)
C00B	-C008	-C00G	117.8(4)	C00J	-C00M	-C00K	120.9(5)
C00B	-C008	-C00I	124.3(4)	C00F	-C00N	-C00Q	120.2(5)
C00G	-C008	-C00I	117.9(4)	C00H	-C00O	-C00L	119.2(5)
C009	-N004	-H004	121.00	C00E	-C00P	-C00Q	121.2(5)
N003	-N004	-H004	121.00	C00N	-C00Q	-C00P	120.7(5)
S001	-C009	-N004	119.3(3)	C005	-C00C	-H00C	120.00
N002	-C009	-N004	123.2(4)	C00J	-C00C	-H00C	120.00
S001	-C009	-N002	117.6(3)	N003	-C00D	-H00D	118.00
C005	-C00A	-C00K	121.3(4)	C00B	-C00D	-H00D	118.00
S001	-C00A	-C005	110.0(3)	C007	-C00E	-H00E	119.00
S001	-C00A	-C00K	128.6(4)	C00P	-C00E	-H00E	119.00
C008	-C00B	-C00D	124.3(4)	C00G	-C00H	-H00H	120.00
C007	-C00B	-C008	118.2(4)	C00O	-C00H	-H00H	120.00

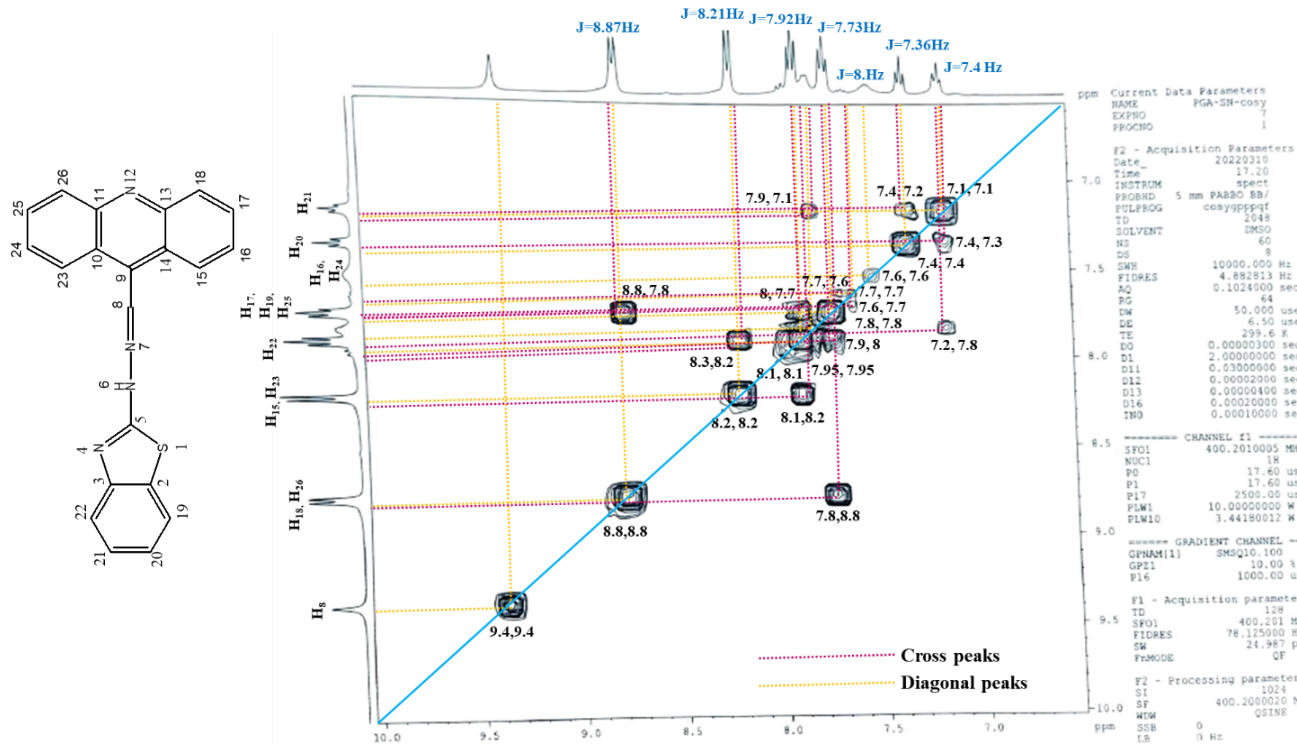


Fig.S3b. ¹H NMR-2D-COSY of ABH in DMSO-d₆

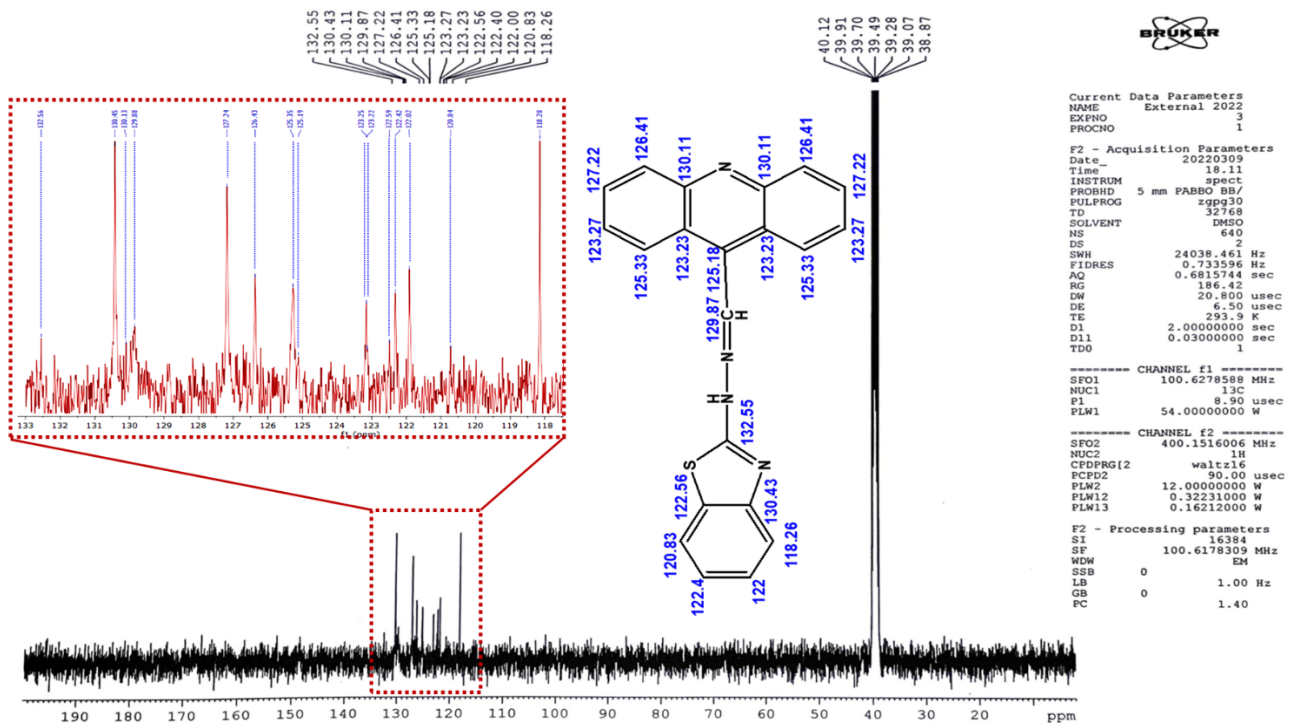


Fig.S3c. ¹³C NMR of ABH in DMSO-d₆

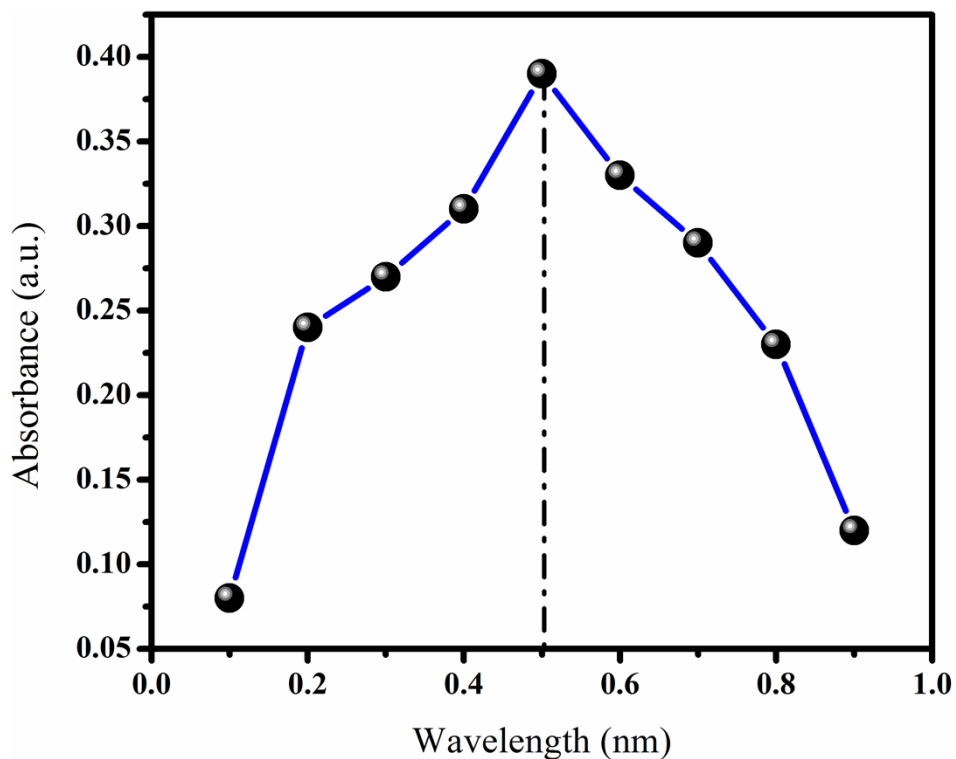


Fig.S4. Job's plot of ABH with As⁺³

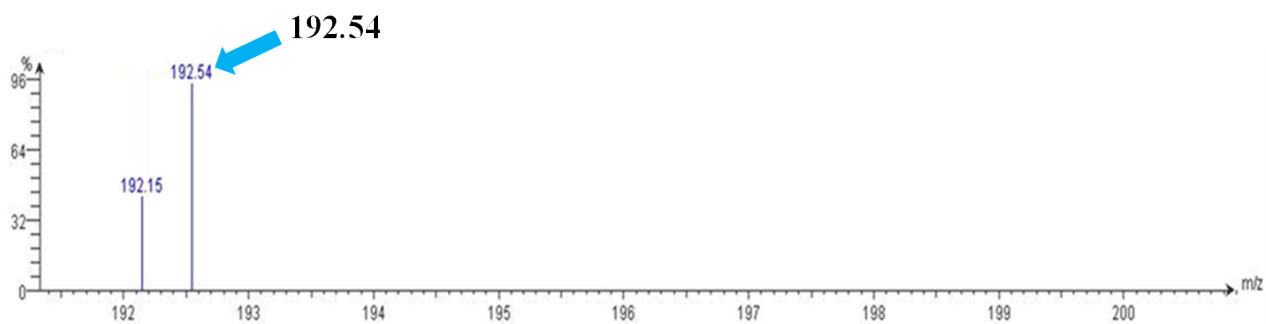
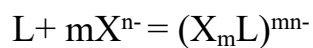


Fig.S5. ESI-Mass data of ABH with As⁺³

Benesi-Hildebrand Equation and Plot

The association constant of a complex formed in between the host molecule and the incoming Metal ion has been determined from the following equilibrium.



$$\frac{(X_mL)^{mn-}}{[L][X^{n-}]^m} = k$$

For 1:1 type complex formation with m=1 following the Benesi-Hildebrand relation, can be expressed in terms of optical density (A) as follows:

$$A = \frac{A_0 + A_1K[X^{n-}]}{1 + K[X^{n-}]}$$

$$\frac{1}{A - A_0} = \frac{1}{A_1 - A_0} + \frac{1}{A_1 - A_0} k [X^{n-}]$$

Where $[X^{n-}]$, $[L]$ and $[(X_mL)^{mn-}]$ are the concentration of the added anions (Here, As^{+3}), host molecule/receptor (here ABH) and the complexation between anions and receptors, respectively. A_0 , A and A_1 indicates the optical density or absorbance at a particular wavelength of receptor 1 or receptor 2 without adding any anion, absorbance after adding anion at every successive step and excess amount of added anion, respectively. The binding constant or association constant K (M^{-1} or M^{-2}) is determined from the ratio of intercept and slope of Benesi-Hildebrand plot of optical density.

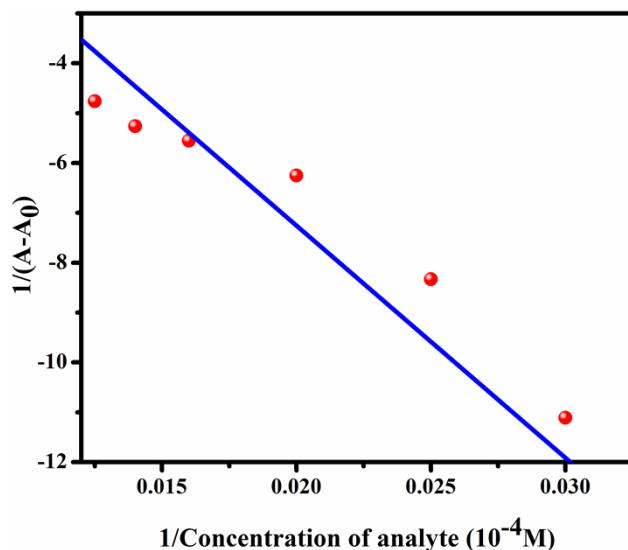


Fig.S6(a). B-H plot of ABH with As³

Detection limit calculation

The detection limit (DL) has been calculated following UV-Vis titration. The absorbance spectrum of ABH was repeated for 5 times, and its standard deviation is measured. The limit of detection (LOD) is calculated from the following formula: $DL = 3\sigma/k$; σ is the standard deviation of the blank solution of ABH. Gradual emergence of new absorbance values during colorimetric titration with targeted analytes is plotted against its concentration. The slope (k) is derived from these plots.

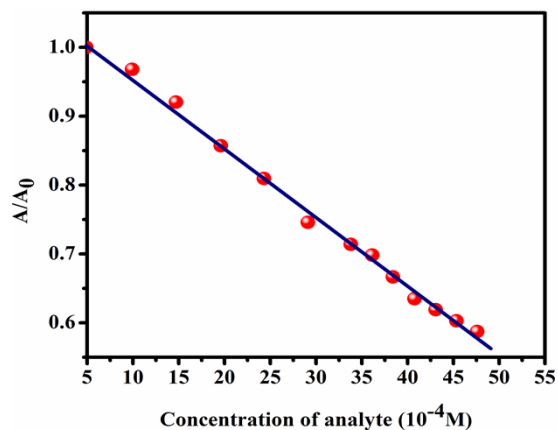


Fig.S6(b).Ratio of absorbance of ABH with As³

Rate constant calculation

Rate constant of the host-guest interaction was calculated from UV-Vis spectroscopy. The sensor and the analytes were taken in similar concentration and the plots of absorbance vs. time were observed in a fixed wavelength. After those three graphs were plotted (i) Absorbance vs. time, (ii) ln Absorbance vs. time and (iii) 1/Absorbance vs. time. Among the three plots, the plot in which the R value is more closed to 1 is chosen and accordingly the order of the reaction was known. Furthermore, the reaction rate was obtained from the slope of the specific plot.

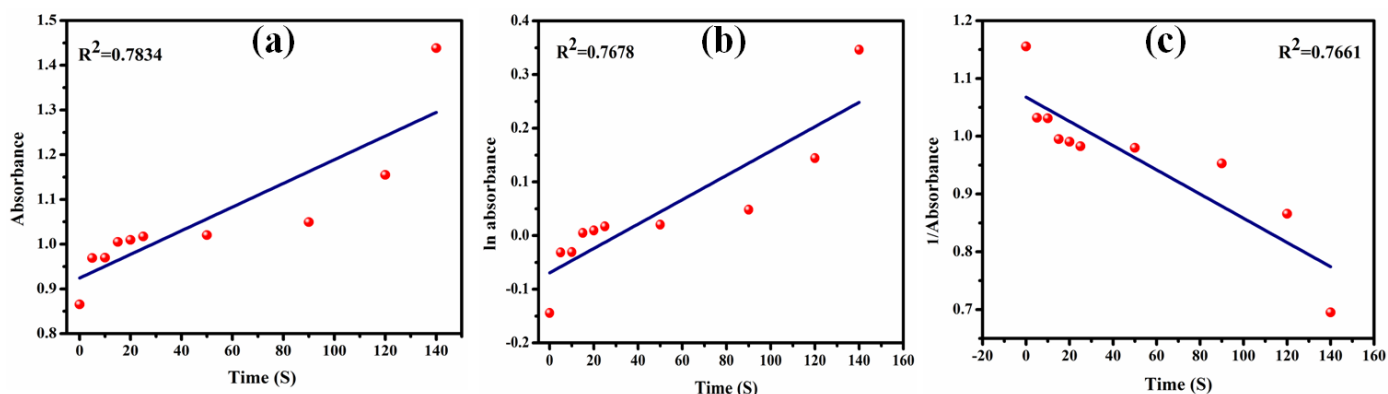
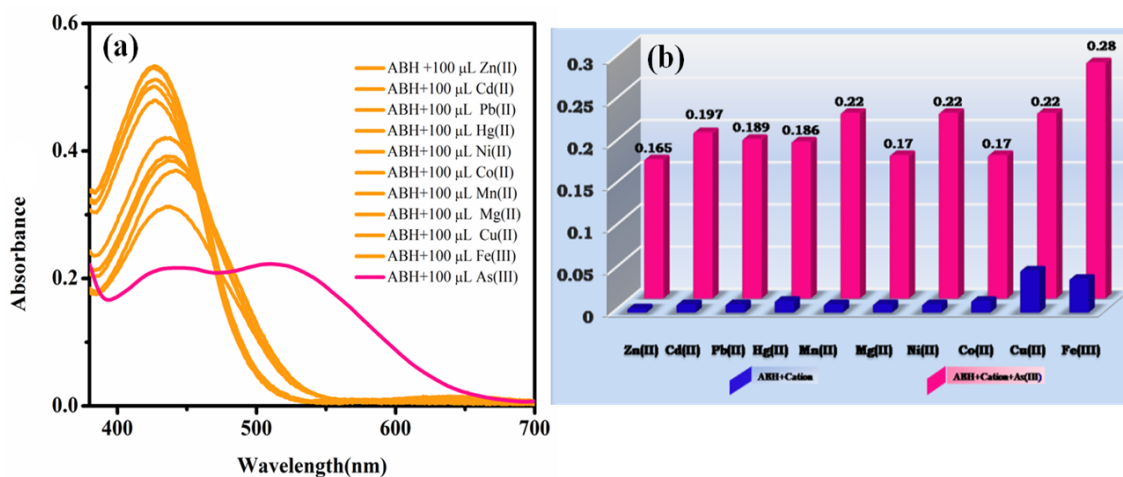


Fig.S7. Plots of Absorbance vs. Time of ABH with As^{+3}



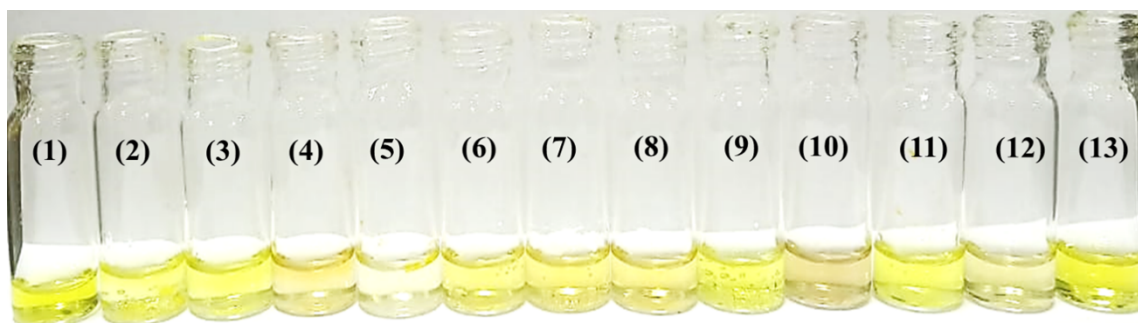


Fig.S8. (a) Absorbance spectra of ABH with different cations, (b) Interference of ABH with different cationic analytes in MeOH-H₂O and (c) Visual colorimetric response of ABH (10⁻⁴M) in methanol in existence of varying cations (10⁻⁴M) in aqueous medium. [Vial 1. ABH (blank), 2. ABH+La³⁺, 3. ABH+Nd³⁺, 4. ABH+Gd³⁺, 5. ABH +Sb³⁺,6. ABH + Sm³⁺, 7. ABH +Al³⁺, 8. ABH +Cr³⁺, 9. ABH +Mg²⁺, 10. ABH +Au³⁺, 11. ABH +Fe³⁺, 12. ABH +Bi³⁺, 13. ABH +Ca²⁺].

Quantitative detection of As⁺³ in terms of RGB values

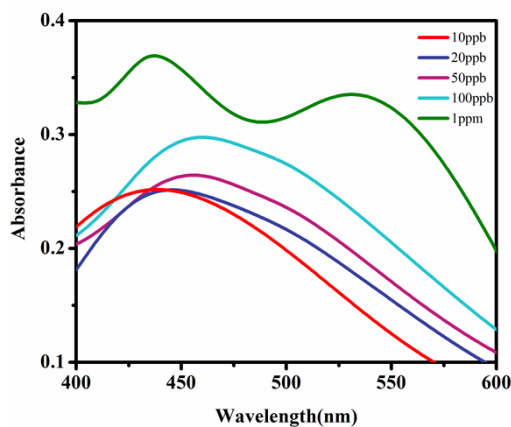


Fig.S9(a). UV-Vis spectra for Quantitative detection of As⁺³ in terms of RGB values

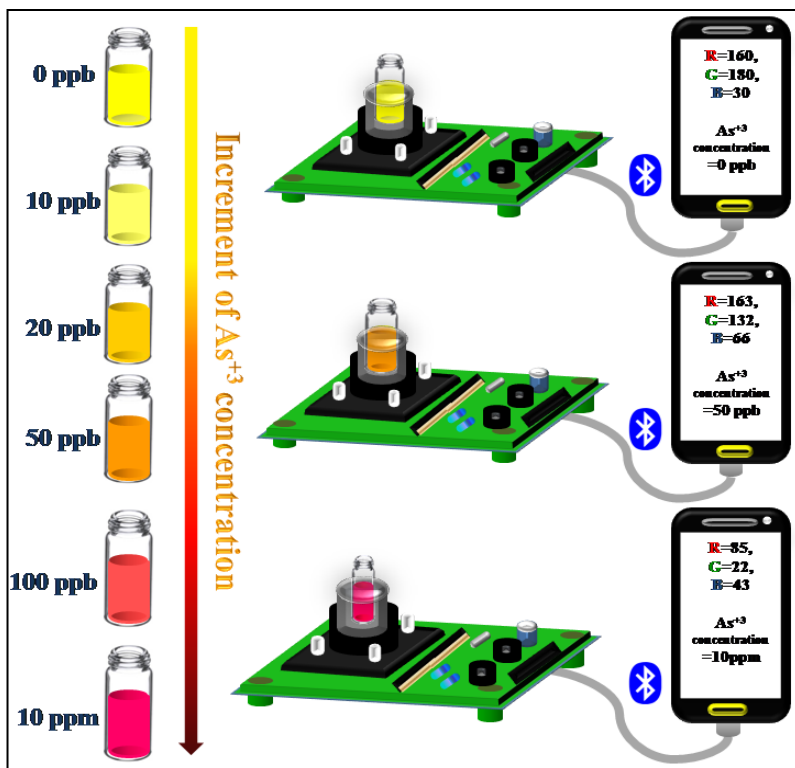


Fig.S9(b).Schematic representation of phone coupled device fabrication for quantitative detection of As³⁺

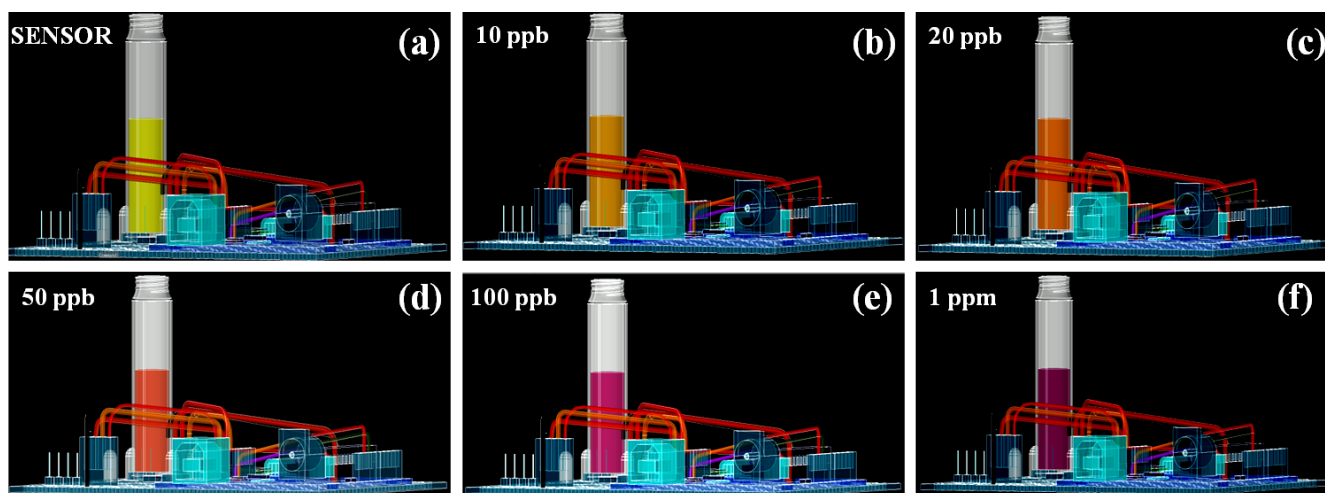


Fig.S10.(a-f).Sensing response of ABH after addition of As³⁺ at different concentration presented in 3D-CAD model

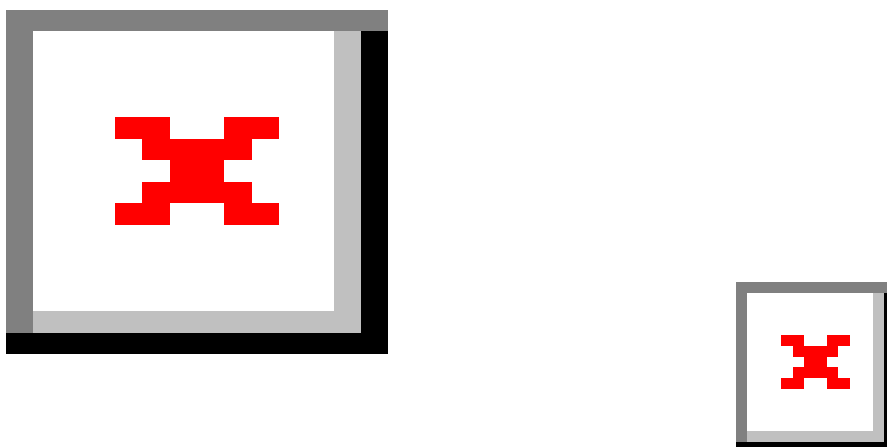


Fig.S11. Fabrication of the logic gate with outputs (Y1 and Y2) upon altering inputs of NAND–NOT–NOR logic functions for ABH with As^{+3} and F^-

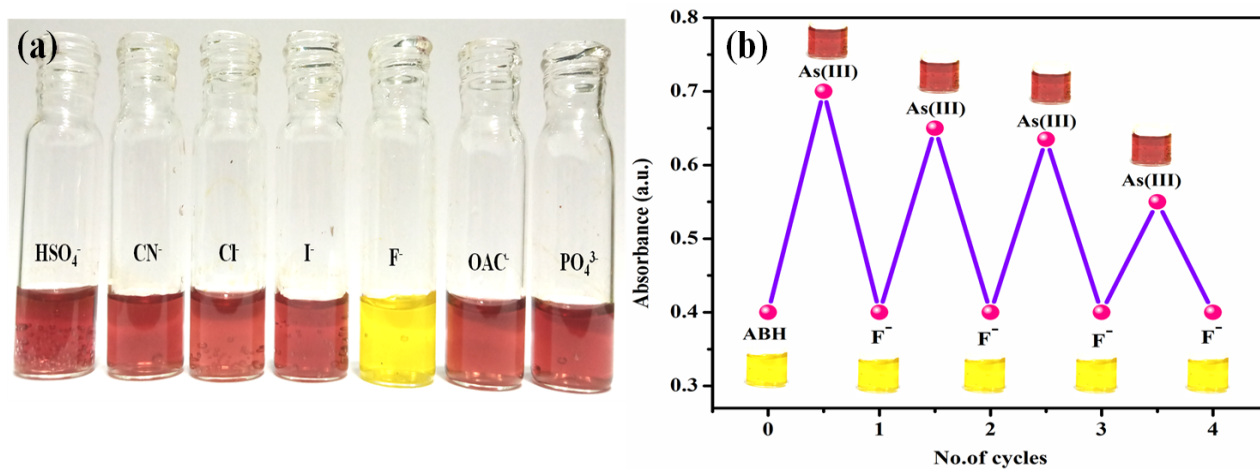


Fig.S12.(a) Visual colour change of [ABH-As³⁺] adduct with F⁻ and other anions and (b) Reversibility ABH with As³⁺ & F⁻ in MeOH

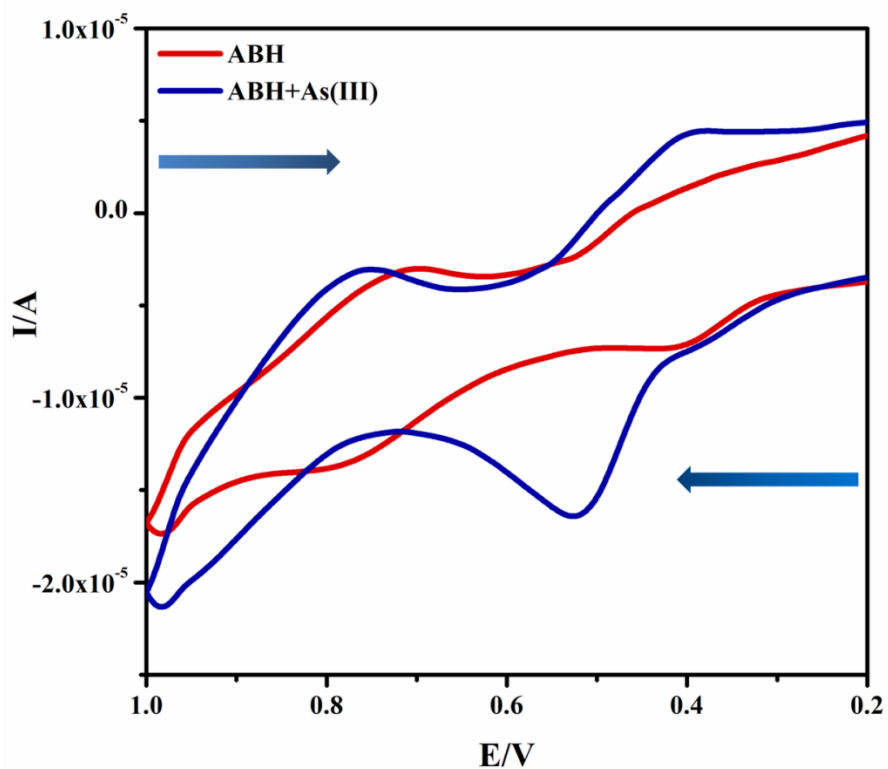


Fig.S13. Electrochemical response of ABH with As^{+3} in MeOH

Table S5 Oxidation Reduction Potential (ORP) of ABH with As^{3+}

	ABH	ABH+(As(III))
Reduction	$E_c = 0.167 \text{ V}$ $I_c = 4.43 \times 10^{-6} \text{ A}$	$E_c = 0.1097 \text{ V}$ $I_c = 5.6 \times 10^{-6} \text{ A}$ $E_c = 0.3915 \text{ V}$ $I_c = 4.43 \times 10^{-6} \text{ A}$
Oxidation	$E_a = 0.413 \text{ V}$ $I_a = -7.395 \times 10^{-6} \text{ A}$ $E_a = 0.775 \text{ V}$ $I_a = -1.36 \times 10^{-5} \text{ A}$	$E_a = 0.519 \text{ V}$ $I_a = -1.645 \times 10^{-5} \text{ A}$

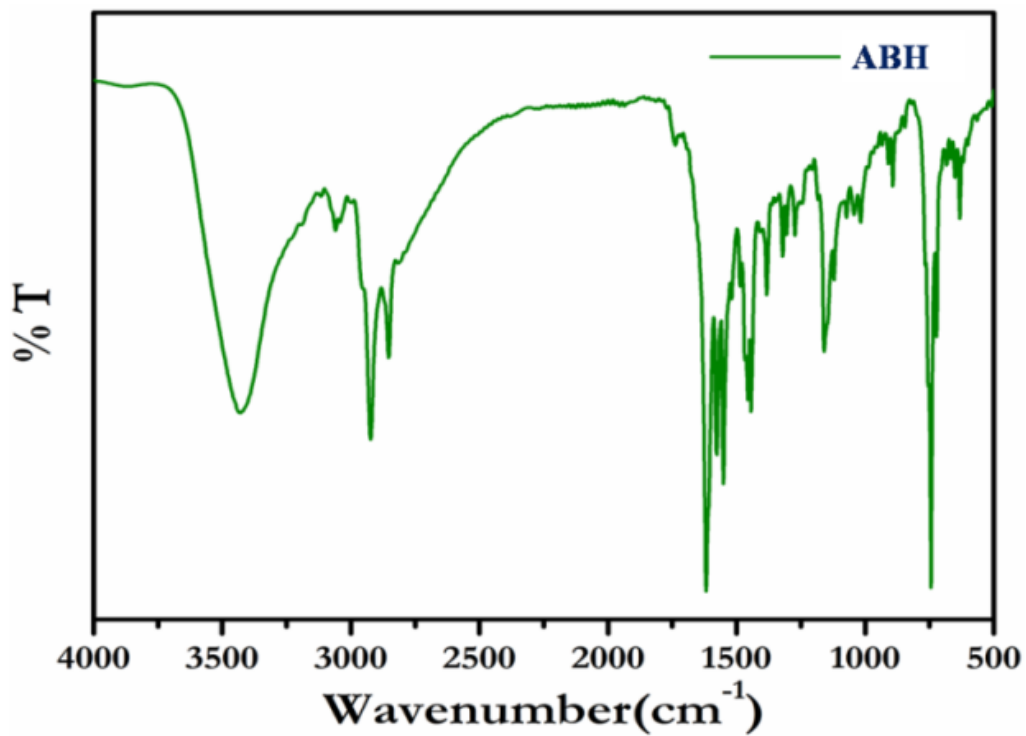


Fig.S14.FT-IR spectra of ABH in solid state

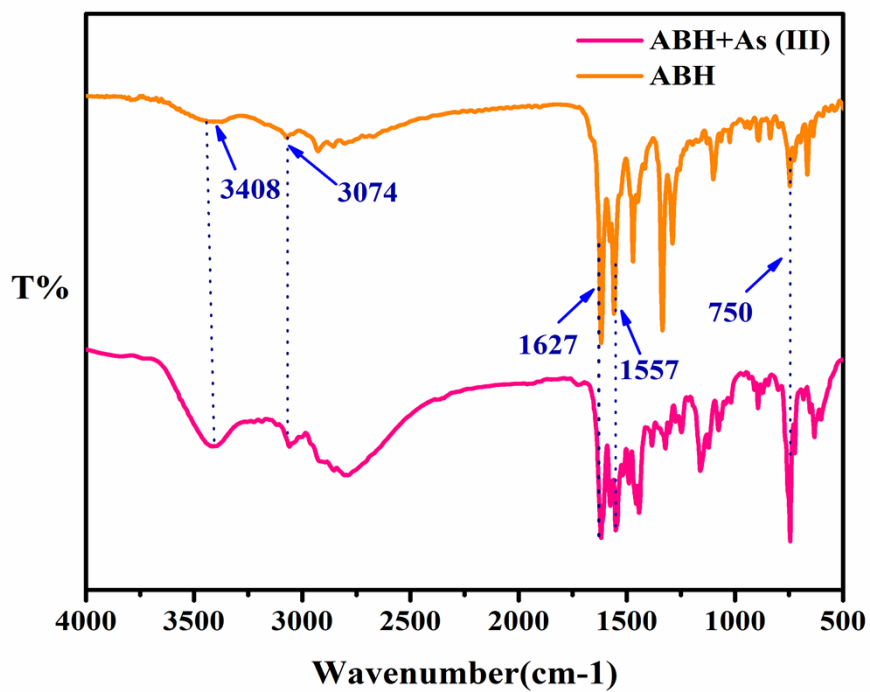


Fig.S15.Infrared spectra of ABH and ABH-As³⁺ adduct

Table S6 Cartesian coordinates of geometry optimized structure of ABH

ATOM		CARTESIAN COORDINATES		
1	s	2.83249083809797	6.35239167139706	53.68841459530811
2	n	7.72335778985233	7.22991852380237	54.04721129502077
3	n	4.58266104411116	4.97026569152620	48.55954499870300
4	n	6.45756741231293	5.73378159685362	50.07263211764133
5	h	8.28774316079637	5.83184058129339	49.44698007151653
6	c	6.69483685459454	7.82628697525408	56.37947093054547
7	n	-0.19180750592023	1.91579036082574	40.56696559385734
8	c	3.77426421839044	3.96768256791613	41.79038649514436
9	c	0.99725677905627	2.20038358841659	45.04520409640357
10	c	5.98072173428171	6.45599880286384	52.50695867909901
11	c	4.04174107216890	7.47865338186203	56.59114661193276
12	c	3.26404071313271	3.50786876674106	44.39845683149521
13	c	8.05177624741146	8.72034950264778	58.48133185117346
14	h	10.09467371479806	8.99316038323325	58.33201500253100
15	c	5.13088209917040	4.36660415583063	46.26220336563216
16	h	7.10389880742531	4.52555947569518	45.62480141375521
17	c	5.96179587007520	5.28600665330664	40.87937743155627
18	h	7.35339741776671	6.02871866526746	42.20650063075953
19	c	1.95541397428020	3.10233751186541	39.93886303952723
20	c	-0.68481469205300	1.46499317239521	43.01131693730174
21	c	-2.99348565982272	0.17172843830957	43.60039360292753
22	h	-4.21984203339087	-0.33158080679869	42.01563406351338
23	c	0.29149959917756	1.50443644305146	47.56695426855312
24	h	1.54430480360085	1.98680171266369	49.12481542626210
25	c	6.75896436619150	9.24230386076756	60.72150003248360
26	h	7.80647766585539	9.93884573610342	62.36318295885189
27	c	2.74229814309555	7.99825924955462	58.83053464466169
28	h	0.69909134786697	7.72109178942812	58.97084148380559
29	c	-1.92956631857728	0.24026724436917	48.05035732097197
30	h	-2.41006341896557	-0.27751973820650	49.99395063598764
31	c	4.12954277766502	8.88534924166400	60.90015265142744
32	h	3.15256974932870	9.30372958337993	62.67405834476605
33	c	2.43006196553968	3.54022714545885	37.30586751678629
34	h	1.01636222398748	2.85018401735857	35.96653861887386
35	c	-3.60980781417536	-0.41715949431923	46.04963620106586
36	h	-5.37283749728763	-1.41103876468477	46.47549311366430
37	c	6.34865796586905	5.67152261725592	38.33728594846797
38	h	8.03688021722704	6.68118059988607	37.70055772260300
39	c	4.56771021484423	4.78143924644129	36.52097186870897
40	h	4.91028639025913	5.10577659017523	34.50745635295921

Table S7 Cartesian coordinates of geometry optimized structure of ABH...As³⁺

ATOM	CARTESIAN COORDINATES		
1 s	2.35175714364505	9.11149722087440	52.34282993126935
2 n	6.00214591658226	5.85633817333158	52.69108095400421
3 n	5.12016231127147	3.00785348328953	48.92925926722882
4 n	3.57557750043754	5.07478130991938	49.22592178570424
5 c	6.35577052293782	7.44606065797380	54.77649400735772
6 n	-0.95228035831601	1.51251553898199	41.31051021636333
7 c	2.56234408347991	3.57387797937587	43.51177996702752
8 c	1.21099854453412	-0.67418419747784	44.76731365133171
9 c	4.02390541972394	6.49528017901022	51.30117725639400
10 c	4.50728984414559	9.36149191524143	54.89255811853522
11 c	2.80797595381760	1.45435192475079	45.14715864181262
12 c	8.24925804538686	7.27765858148470	56.61190739120907
13 c	4.72177060123413	1.32711453287003	47.14031148288026
14 c	4.22070897560514	5.71251060447650	43.54030257457010
15 c	0.57783861671163	3.50387040178166	41.62612041304936
16 c	-0.65729835488984	-0.53399129645859	42.77542525789239
17 c	-2.29212563053160	-2.65307239355026	42.35887207842038
18 c	1.31067151186952	-2.91193341347544	46.28045319103641
19 c	8.24636589203199	9.06022056872397	58.55618315401242
20 c	4.50413780965660	11.14438846612621	56.83751553854261
21 c	-0.28755112240626	-4.91001889399090	45.81319134338853
22 c	6.39945311333293	10.96871689508188	58.66888808627577
23 c	0.25627594277018	5.63318305036791	39.98025908824744
24 c	-2.10659317428215	-4.78467414716273	43.82706735728953
25 c	3.86449320963175	7.70374959504811	41.90695746450780
26 c	1.84118216273957	7.68120473319256	40.12477707461763
27 as	7.87339980704549	2.94709535667732	51.43499724695475
28 h	1.92551689768065	5.13795925850792	48.23072197292947
29 h	9.68555918616333	5.79452821796665	56.53049919147805
30 h	5.94400111199733	-0.33510342500731	47.27582600827787
31 h	5.82498252649015	5.75212902164851	44.83951747026612
32 h	-3.67927540463676	-2.49362769741946	40.83692369783858
33 h	2.65668187591522	-3.03682162122623	47.84133299314600
34 h	9.70747597855408	8.96442462712499	60.01418610609397
35 h	3.06993304446478	12.62717684037198	56.92845027885223
36 h	-0.17680893202007	-6.60974191874781	46.98487623122993
37 h	6.44037922600826	12.34114352686781	60.21316100829977
38 h	-1.27556041426524	5.53486021898886	38.59815406271444
39 h	-3.36210142002085	-6.39320187825166	43.49291337877192
40 h	5.16063822205379	9.31356580090942	41.95531565967185
41 h	1.58665067199842	9.29045151704256	38.85180559710409
42 i	9.06128256234929	-13.50936465425681	69.72396019186904
43 i	10.76118288399203	-14.37838144985135	75.08443255905078
44 i	7.35860872676249	-12.63862912802591	64.35234153677563

Table S8 Loewdin population analysis plot

	Loewdin atomic charges of ABH	Loewdin atomic charges of ABH...As³⁺
1s	0.139	0.363
2n	-0.143	0.3962
3n	-0.154	0.3507
4n	-0.0206	-0.083
5c	-0.09	0.01859
6n	-0.027	-0.04619
7c	-0.024	-0.0099
8c	-0.045	-0.00323
9c	0.008	0.03573
10c	-0.201	-0.08420
11c	-0.1745	0.01247
12c	-0.1829	-0.1728
13c	-0.00106	-0.00529
14c	-0.00052	-0.1644
15c	-0.18619	0.0130
16c	-0.18440	0.01677
17c	-0.18359	-0.1225
18c	-0.19027	-0.1515
19c	-0.18275	-0.1469
20c	-0.193	-0.15606
21c	-0.182	-0.12327
22c	-0.1753	-0.15226
23c	-0.1753	-0.13272
24c	-0.177	-0.13836
27As	-	-0.707
28i	-	1

29i	-	0.9
30i	-	0.2939

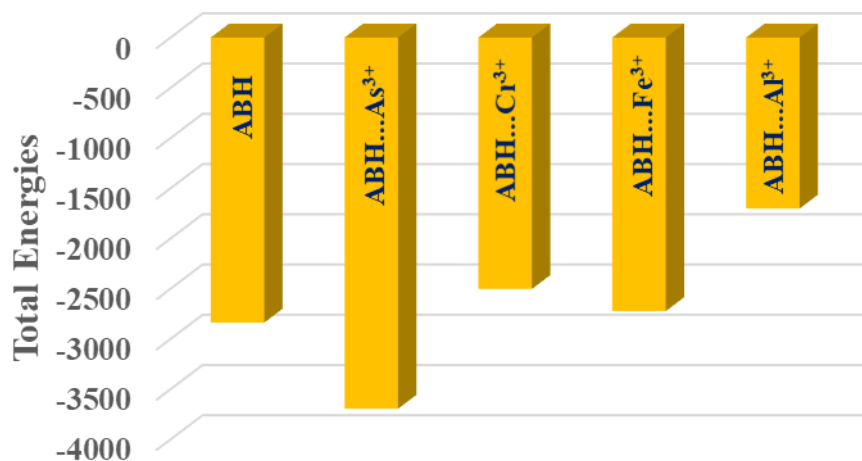


Fig.S16.Interaction of **ABH** with lethal interfering trivalent cations

Table S9 2D-COSY analysis of **ABH**

¹ H- ¹ H diagonal peak (ppm)	¹ H- ¹ H cross peak (ppm)
9.4-9.4	7.8-8.8
8.8-8.8	8.1-8.2
8.2-8.2	8.8-7.8
8.1-8.1	8.3-8.2
7.95-7.95	7.9-8
7.8-7.8	7.2-7.8
7.7-7.7	7.6-7.7
7.6-7.6	7.4-7.3
7.4-7.4	7.2-7.4
7.1-7.1	7.9-7.1

Table S10 Comparative literature study of **ABH** with other chemosensors

Sl. no	Analytes detected	Sensor	LOD	Logic gate ensemble	Device fabrication	Aqueous phase 'Naked eye' detection	Removal of targeted analyte	Ref.
--------	-------------------	--------	-----	---------------------	--------------------	-------------------------------------	-----------------------------	------

1.	As ⁵⁺	Polypyrrole-chitosan-cobalt ferrite nanoparticles	1ppb	-	-	Yes	-	31
2.	Al ³⁺ , Fe ³⁺ , Cr ³⁺ , As ³⁺ , In ³⁺ Ga ³⁺	Thiourea based probe	.01ppb	-	-	Yes	-	32
3.	As ³⁺	Graphite pencil electrode modified with tin oxide nanoneedles	10 ppb	-	-	-	-	33
4.	As ³⁺ , As ⁵⁺	semi-automated portable sensor device	3ppb	-	Yes	Yes	-	34
5.	As ³⁺ As ⁵⁺	Benzothiazole functionalized Schiff Base probe	7.2 ppb 6.7 ppb	-	Yes	Yes	-	35
6.	As ³⁺	Coumarin based probe	0.24 ppb	-	-	-	-	36
7.	As ³⁺	Au-NP based Colorimetric and Ultrasensitive Dynamic Light Scattering Assay	3ppb	-	-	Yes	-	37
8.	As ⁵⁺	Bimetallic Nanoparticles based probe	1.2 ppb	-	-	Yes	-	7
9.	As ³⁺	SERS based Glutathione Functionalized Silver Nanoparticle	0.76 ppb	-	-	Yes	-	38
10.	As ³⁺	Cationic polymers and aptamers mediated	5.3 ppb	-	-	Yes	-	39

		aggregated gold nanoparticles						
11.	As³⁺	Benzothiazole functionalized Schiff base molecule	5.4 ppb	Yes [ABH... As ³⁺ exhibits ~5 times selective reversibility with F ⁻ : Fabrication of logic-gate]	Yes [Bluetooth operated RGB based portable smartphone ensembled POCT device]	Yes [Aqueous phase chromomeric semi quantitative detection]	Yes [Metal complex based mitigation of As ³⁺]	ABH